

STOCHASTIC TRUNCATED WIRTINGER FLOW ALGORITHM FOR PHASE RETRIEVAL USING BOOLEAN CODED APERTURES

Samuel Pinilla, Camilo Noriega, Henry Arguello

Computer Science Department, Universidad Industrial de Santander
Bucaramanga, Colombia 680002
{samuel.pinilla,camilo.noriega}@correo.uis.edu.co, henarfu@uis.edu.co

ABSTRACT

X-ray crystallography is an experimental technique to estimate the 3D atomic positions of the elements present in a crystal. This technique constructs the 3D structure from the phase of diffracted and patterned X-rays (DPX). Multiple intensity DPX measurements are acquired to solve the phase retrieval problem. The feasibility of implementing this technique depends on solving the phase retrieval problem using expensive multiple valued patterns and the Truncated Wirtinger Flow Algorithm. This paper presents a Stochastic Truncated Wirtinger Flow Algorithm (STWF) which solves the phase retrieval problem based on DPX measurements low-cost boolean block-unblock coded apertures. Several simulations are realized to demonstrate the convergence of the STWF algorithm and the optimal parameters of the boolean coded apertures. The results indicate that given the DPX measurements, the quality of reconstructed phase images using STWF attained up 24.63dB of PSNR.

Index Terms— X-ray crystallography, coded aperture, phase retrieval, diffraction pattern.

1. INTRODUCTION

X-ray crystallography allows determining the atomic position of a crystal in a three-dimensional (3D) space using the phase of optically sensed diffraction patterns [1]. The 3D model is valuable in applications such as the design of medicines [2] and the development of new materials [3]. However, optical sensors cannot directly measure the phase of the diffraction patterns. Therefore, it must be recovered from the acquired diffraction patterns of the crystal under study. Furthermore, the use of a coding element in the X-ray sensing system was proposed in [4], in order to reduce the exposition to x-ray of the crystal encoding and modulating the diffraction patterns. Particularly, recently proposed coding designs [5, 6, 7] modulate the X-ray diffraction patterns changing their phase or blocking some diffracted beams before being measured in the sensor. The percentage of unblocked coded X-ray diffraction beams is known as the transmittance of the coding element. Several methods as described in [5, 6, 8] allow to recover the phase from the coded X-ray diffraction patterns. Some

of them include the non-convex formulations of the phase retrieval problem via Truncated Wirtinger Flow (TWF) [6, 8]. In addition, these works have proposed coding elements that help in obtaining the reconstruction of the phase. Despite the fact that the state-of-the-art octanary codification pattern designs in [4] allow to recover the phase from diffracted beams, their physical implementation in a real architecture is highly expensive, because it requires finding a material to change the phase of a diffracted beam.

In contrast, this work presents a Stochastic Truncated Wirtinger Flow Algorithm (STWF) which solves the phase retrieval problem based on DPX measurements acquired with low-cost boolean block and unblock coded apertures. Boolean coded apertures refer to those designs in which each element blocks or lets pass through the X-ray diffracted beams. The performance of the STWF algorithm is analyzed in this paper when different boolean code designs are used. Simulations show that the quality of the reconstructions using boolean coded apertures attained up 24.63dB of PSNR and their construction in a real diffraction pattern system is feasible in comparison with the octanary pattern designs. In addition, the results show that the optimal transmittance for the coded aperture designs is around 50%.

2. PHASE RETRIEVAL FROM ENCODED DIFFRACTION PATTERNS

The measurements in the phase retrieval problem are given by

$$y_k = |\langle \mathbf{a}_k, \mathbf{x} \rangle|^2, k = 1, \dots, n, \quad (1)$$

where $\mathbf{a}_k \in \mathbb{C}^n$ are the row vectors in the Fourier Transform matrix $\mathbf{F} = [\mathbf{a}_1, \dots, \mathbf{a}_n]^* \in \mathbb{C}^{n \times n}$, $\mathbf{x} \in \mathbb{C}^n$ is unknown [6] and $*$ is the Hermitian transpose operation. Let $\mathbf{y} = [y_1, \dots, y_n]^* \in \mathbb{R}^n$ be the measurements vector, such that Equation (1) can be rewritten as

$$\mathbf{y} = |\mathbf{F}\mathbf{x}|^2 \quad (2)$$

where $|\cdot|$ is the pointwise magnitude. Moreover, considering noise in the observed measurements, they can be modeled as $y_k \sim \text{Poisson}(|\langle \mathbf{a}_k, \mathbf{x} \rangle|^2)$, $k = 1, \dots, n$. Note that $|\langle \mathbf{a}_k, \mathbf{x} \rangle|^2 = (\mathbf{a}_k^* \mathbf{x})(\mathbf{a}_k^* \mathbf{x})^* = \mathbf{a}_k^* (\mathbf{x}\mathbf{x}^*) \mathbf{a}_k$, where $\mathbf{X} = \mathbf{x}\mathbf{x}^*$ is a rank-one matrix. Considering a stochastic noise model with independent samples and seeking the maximum likelihood estimate (MLE), the recovery problem is given by

$$\begin{aligned}
& \underset{\mathbf{x} \in \mathbb{C}^n}{\text{argmin}} && \sum_{k=1}^n \mu_k^2 - y_k \log(\mu_k) + \lambda \text{Tr}(\mathbf{X}) \\
& \text{subject to} && \mu_k = \mathbf{a}_k^* \mathbf{X} \mathbf{a}_k, \quad k = 1, \dots, n, \\
& && \mathbf{X} \succeq 0.
\end{aligned} \tag{3}$$

The optimization problem in Eq. (3) can be solved with the TWF algorithm which is a gradient descent method [6]. The TWF algorithm was used in [6] to recover the phase when the architecture includes an optical element known as octanary coding element. This element modulates the X-ray diffraction pattern before being measured in the sensor. More specifically, the measurements of the detector in Eq. (2) considering the effect of the coding element are given by

$$\mathbf{y} = |\mathbf{F}\mathbf{D}\mathbf{x}|^2 \tag{4}$$

where $\mathbf{D} \in \{1, -1, j, -j\}^{n \times n}$ is a diagonal matrix that represents the octanary patterns. Note that the coded diffraction measurements in Eq. (4) can be considered as a single projection. Thus, let L be the number of projections and \mathbf{D}^ℓ be a different coding pattern corresponding to each projection, then multiple projections, each with different pattern can be written as

$$\mathbf{y}^\ell = |\mathbf{F}\mathbf{D}^\ell \mathbf{x}|^2. \tag{5}$$

Despite the fact that octanary coding patterns have been designed to recover the phase from diffracted beams, its physical implementation in a real architecture is impractical because it requires changing the phase of a diffracted beam and finding a material allowing this characteristic is highly expensive.

Algorithm 1 Stochastic Truncated Wirtinger Flow Algorithm

```

1: function STWF-ALGORITHM ( $\alpha_0, \alpha_1, \alpha_2, \alpha_3, \mathbf{y}, T$ )
2:    $\{\mathbf{a}_k \in \mathbb{C}^n | 1 \leq k \leq n\}$  (Sampling vectors)
3:    $\lambda_0 \leftarrow \sqrt{\frac{1}{n} \sum_{k=1}^n y_k}$ 
4:    $\mathbf{H} \leftarrow \frac{1}{n} \sum_{k=1}^n y_k \mathcal{F}(\mathbf{a}_k \mathbf{a}_k^*) \mathbf{1}_{\{|y_k| \leq \alpha_3 \lambda_0^2\}}$ 
5:    $\mathbf{x}^{(0)} \leftarrow \sqrt{\frac{n^2}{\sum_{k=1}^n \|\mathbf{a}_k\|^2}} \lambda_0 \bar{\mathbf{x}}$  ( $\bar{\mathbf{x}}$  is the leading eigenvector of  $\mathbf{H}$ )
6:   for  $t = 1$  to  $T$  do
7:      $\mathbf{x}^{(t+1)} \leftarrow \mathbf{x}^{(t)} + \frac{2\mu_t}{n} \sum_{k=1}^n \underbrace{\frac{(y_k - |\mathbf{a}_k^* \mathbf{x}^{(t)}|^2)}{\mathbf{x}^{(t)H} \mathbf{a}_k}}_{v^k} \mathbf{a}_k \mathbf{1}_{\epsilon_1^k} \cap \epsilon_2^k$ 
8:     where:
9:      $\epsilon_1^k \leftarrow \{\alpha_0 \leq \frac{\sqrt{n} |\mathbf{a}_k^* \mathbf{x}^{(t)}|}{\|\mathbf{a}_k\| \|\mathbf{x}^{(t)}\|} \leq \alpha_1\}$ 
10:     $\epsilon_2^k \leftarrow \{|y_k - |\mathbf{a}_k^* \mathbf{x}^{(t)}|^2| \leq \frac{\alpha_2 K_t \sqrt{n} |\mathbf{a}_k^* \mathbf{x}^{(t)}|}{\|\mathbf{a}_k\| \|\mathbf{x}^{(t)}\|}\}$ 
11:     $K_t \leftarrow \frac{1}{n} \sum_{k=1}^n |y_k - |\mathbf{a}_k^* \mathbf{x}^{(t)}|^2|$ 
12:   end for
13:    $l \leftarrow \sum_{k=1}^n (y_k \log(|\langle \mathbf{a}_k, \mathbf{x}^{(T)} \rangle|^2) - |\langle \mathbf{a}_k, \mathbf{x}^{(T)} \rangle|^2)$ 
14:   return  $\mathbf{x}^{(T)}, l$ 
15: end function

```

In contrast, the block-unblock coded apertures presented in this work, known as boolean coded apertures, can be easily implemented in X-ray diffraction applications [9] and [10].

Moreover, the blocking elements of these coded apertures can be fabricated using tungsten powder, because this material can stop an x-ray diffracted beam, resulting in low fabrication cost [10, 11].

The TWF algorithm cannot be directly applied to recover the phase from boolean coded aperture measurements. Therefore, this work presents a Stochastic Truncated Wirtinger Flow Algorithm (STWF), described in Algorithm 1, which uses a feasible modulation of the diffraction patterns based on boolean coded apertures. The first modification consists on simulating a coding pattern with $\{-1, 1\}$ elements using boolean coded apertures which is explained in Section 4. The second modification is to change the initialization of $\mathbf{x}^{(0)}$ in Algorithm 1 line 5, which is the leading

eigenvector of the matrix $\mathbf{H} = \frac{1}{n} \sum_{k=1}^n y_k \mathbf{a}_k \mathbf{a}_k^* \mathbf{1}_{\{|y_k| \leq \alpha_3 \lambda_0^2\}}$. The TWF algorithm in [6] considers that the sampling vectors \mathbf{a}_k in a general case, are normally distributed, *i.e.* $\mathbf{a}_k \sim \mathcal{N}(0, \mathbf{I}) + i\mathcal{N}(0, \mathbf{I}), k = 1, \dots, n$. However, in the X-ray phase retrieval problem case, these vectors are the rows of the Discrete Fourier Transform Matrix. Then, given that gradient descent methods highly depend on the initial guess and in order to get the initialization of $\mathbf{x}^{(0)}$ in the Fourier domain, the matrix \mathbf{H} in Algorithm 1 line 4, was initialized as

$$\mathbf{H} = \frac{1}{n} \sum_{k=1}^n y_k \mathcal{F}(\mathbf{a}_k \mathbf{a}_k^*) \mathbf{1}_{\{|y_k| \leq \alpha_3 \lambda_0^2\}}, \tag{6}$$

where $\mathcal{F}(\cdot)$ represents the Fourier Transform. In Algorithm 1 the inputs $\alpha_0, \alpha_1, \alpha_2$ and α_3 in line 1, are the truncation parameters. The terms $\epsilon_1^k, \epsilon_2^k$ defined in line 9 and 10, respectively, are two collections of events *i.e.* the value of ϵ_1^k and ϵ_2^k is 1 when their respective constraint is satisfied and 0 otherwise. Moreover, the notation of truncation $\epsilon_1^k \cap \epsilon_2^k$ simply to discard the values v^k in line 7 when $\epsilon_1^k \cap \epsilon_2^k = \emptyset$. Then, the action of $|y_k| \leq \alpha_3 \lambda_0^2$ in the initialization of \mathbf{H} in line 4, is to discard those measurements that are several times larger than the average [6]. The returned variable l in line 14 is the log-likelihood of the solution $\mathbf{x}^{(T)}$. Finally, since the STWF algorithm is a truncated gradient descent method, the truncation parameters limit the adequate search area to find the solution. Thus, the optimal values of the truncation parameters $\alpha_0, \alpha_1, \alpha_2$ and α_3 are calculated using a Markov Chains Monte Carlo method (MCMC) presented in Section 5.

3. BOOLEAN CODED APERTURE DESIGNS

The boolean coded aperture theoretically is designed as a diagonal matrix $\mathbf{D} = (d_{kk}) \in \{0, 1\}^{n \times n}$, where $d_{kk} = 1$ represents a transmissive element and $d_{kk} = 0$ represents a blocking element. Moreover, the transmittance of the boolean coded aperture is defined as $t_r = \sum_{k=1}^n \sum_{j=1}^n \frac{d_{k,j}}{n^2}$.

Figure 1 shows an example of different boolean coded aperture designs, where the white elements indicate one-value entries that allow the beams to pass through and the black elements are 0 in the coded aperture design. Figure 1(a) shows

a blue noise pattern in which cluster of ones and zeros are easily noticeable. To reduce these clusters occurrences, blue noise patterns [12] are used as illustrated in Fig. 1(b). Other types of boolean coded apertures include the Hadamard and DFT matrices shown in Fig. 1(c) and Fig 1(d), respectively.

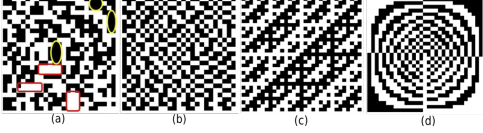


Fig. 1: Coded aperture designs with 32×32 pixels and 50% of transmittance. (a) Random coded aperture. (b) Coded aperture with blue noise pattern. (c) Hadamard coded aperture. (d) Coded aperture based on DFT

4. CONVERGENCE OF THE STWF ALGORITHM USING BOOLEAN CODING

First, the convergence of the STWF algorithm is presented for coding elements $\{-1, 1\}$. After, it is illustrated that the measurements based on $\{-1, 1\}$ codification can be implemented via boolean coded apertures. In order to analyze the modulation elements $\{-1, 1\}$ of the x-ray diffraction patterns with the STWF algorithm, consider the following lemma.

Lemma 4.1. *Let $A \sim \mathcal{N}(0, 1)$ and consider a random variable B independent of A such that*

$$Pr(\mathcal{B} = b) = \begin{cases} \frac{1}{2} & \text{if } b = 1 \text{ or } b = -1 \\ 0 & \text{otherwise} \end{cases}$$

then $C = AB$ is a Gaussian random variable and $C \sim \mathcal{N}(0, 1)$.

The TWF algorithm in [6] considers that the sampling vectors in Equation (1) are normally distributed, *i.e.* $\mathbf{a}_k \sim \mathcal{N}(0, \mathbf{I}) + i\mathcal{N}(0, \mathbf{I})$, $k = 1, \dots, n$. On the other hand, let \mathbf{E} be a diagonal matrix with $\{-1, 1\}$ coding elements. Thus, considering Lemma (4.1) the resulting vector $\mathbf{E}\mathbf{a}_k$ is normally distributed as \mathbf{a}_k . Moreover, since the convergence of the TWF algorithm, is guaranteed in [6], using normally distributed sampling vectors, a coding pattern based on $\{-1, 1\}$ elements is a feasible modulation. To illustrate how the measurements based on $\{-1, 1\}$ coding elements can be implemented by using boolean coded apertures, note that these measurements can be written as

$$y_k^\ell = |\langle \mathbf{E}^\ell \mathbf{a}_k, \mathbf{x} \rangle|^2, k = 1, \dots, n, \ell = 1, \dots, L, \quad (7)$$

where $\mathbf{E}^\ell \in \{-1, 1\}^{n \times n}$ is a diagonal matrix. Note that $(\mathbf{E}^\ell + \mathbf{I})/2 = \mathbf{D}^\ell$ is a boolean coded aperture, where \mathbf{I} is the identity matrix. Notice that $\mathbf{I} = (\mathbf{I} - \mathbf{D}^\ell) + \mathbf{D}^\ell$ and $2\mathbf{D}^\ell - \mathbf{I} = \mathbf{E}^\ell$, then defining the $\overline{\mathbf{D}}^\ell = \mathbf{I} - \mathbf{D}^\ell \in \{0, 1\}^{n \times n}$ matrix, the identity can be rewritten as $\mathbf{I} = \mathbf{D}^\ell + \overline{\mathbf{D}}^\ell$ and Equation (7) can be expressed as

$$\begin{aligned} y_k^\ell &= |\langle (\mathbf{D}^\ell - \overline{\mathbf{D}}^\ell) \mathbf{a}_k, \mathbf{x} \rangle|^2 \\ &= \mathbf{x}^* ((\mathbf{D}^\ell - \overline{\mathbf{D}}^\ell) \mathbf{a}_k \mathbf{a}_k^* (\mathbf{D}^\ell - \overline{\mathbf{D}}^\ell)) \mathbf{x} \\ &= \mathbf{x}^* (\mathbf{D}^\ell \mathbf{a}_k \mathbf{a}_k^* \mathbf{D}^\ell) \mathbf{x} + \mathbf{x}^* (\overline{\mathbf{D}}^\ell \mathbf{a}_k \mathbf{a}_k^* \overline{\mathbf{D}}^\ell) \mathbf{x} \\ &\quad - \underbrace{\mathbf{x}^* (\overline{\mathbf{D}}^\ell \mathbf{a}_k \mathbf{a}_k^* \mathbf{D}^\ell + \mathbf{D}^\ell \mathbf{a}_k \mathbf{a}_k^* \overline{\mathbf{D}}^\ell) \mathbf{x}}_{\mathbf{v}}. \end{aligned} \quad (8)$$

Using the fact that $\overline{\mathbf{D}}^\ell = \mathbf{I} - \mathbf{D}^\ell$ and $\mathbf{D}^\ell = \mathbf{I} - \overline{\mathbf{D}}^\ell$ the term \mathbf{V} in Equation (8) can be alternatively expressed as

$$\begin{aligned} \mathbf{V} &= (\mathbf{I} - \mathbf{D}^\ell) \mathbf{a}_k \mathbf{a}_k^* \mathbf{D}^\ell + (\mathbf{I} - \overline{\mathbf{D}}^\ell) \mathbf{a}_k \mathbf{a}_k^* \overline{\mathbf{D}}^\ell \\ &= \mathbf{a}_k \mathbf{a}_k^* - (\mathbf{D}^\ell \mathbf{a}_k \mathbf{a}_k^* \mathbf{D}^\ell + \overline{\mathbf{D}}^\ell \mathbf{a}_k \mathbf{a}_k^* \overline{\mathbf{D}}^\ell) \end{aligned} \quad (9)$$

Using the above equivalence of matrix \mathbf{V} , Equation (8) can be expressed in equivalent form as

$$y_k^\ell = 2(|\langle \mathbf{D}^\ell \mathbf{a}_k, \mathbf{x} \rangle|^2 + |\langle \overline{\mathbf{D}}^\ell \mathbf{a}_k, \mathbf{x} \rangle|^2) - |\langle \mathbf{a}_k, \mathbf{x} \rangle|^2. \quad (10)$$

From Equation (10), the encoded diffraction patterns based on $\{-1, 1\}$ modulation elements in matrix form, can be written as

$$\mathbf{y}^\ell = |\mathbf{F}(2\mathbf{D}^\ell - \mathbf{I})\mathbf{x}|^2 = 2(|\mathbf{F}\mathbf{D}^\ell\mathbf{x}|^2 + |\mathbf{F}\overline{\mathbf{D}}^\ell\mathbf{x}|^2) - |\mathbf{F}\mathbf{x}|^2. \quad (11)$$

Remark that the three terms in Equation (11) can be implemented by using boolean coded apertures.

5. ESTIMATION METHOD FOR TRUNCATED PARAMETERS

Algorithm 2 is an implementation of Metropolis Hasting Algorithm to determine the truncation parameters of STWF algorithm, using the sampling Markov Chains Monte Carlo method (MCMC). Since that the optimal truncation parameters values α_j of STWF algorithm cannot be determine in an analytical way, the MCMC algorithms is a numerical alternative for estimate them. For all experiments, prior distributions were assumed over truncation parameters $\alpha_j \in \mathbf{p}$ (with zero probability for negative values). In the MCMC scheme, for

Algorithm 2 Metropolis Hasting Algorithm

```

1: function MCMC-ALGORITHM ( $\mathbf{y}, M, \sigma_0, \sigma_1, \sigma_2, \sigma_3, T$ )
2:    $\alpha_0 \leftarrow 0.1, \alpha_1 \leftarrow 2.5, \alpha_2 \leftarrow 3, \alpha_3 \leftarrow 1300$ 
3:    $\mathbf{p} \leftarrow [\alpha_0, \alpha_1, \alpha_2, \alpha_3]$ 
4:    $l^{(0)} \leftarrow \text{STWF-ALGORITHM}(\mathbf{p}, \mathbf{y}, T)$ 
5:    $\mathbf{L}_{(0,:)} \leftarrow \mathbf{p}$ 
6:   for  $t = 0$  to  $M$  do
7:      $a \leftarrow (t \bmod 4)$ 
8:      $\mathbf{p}_{(a)} \leftarrow \log\mathcal{N}(\alpha_a, \sigma_a)$ 
9:      $l^{(t+1)} \leftarrow \text{STWF-ALGORITHM}(\mathbf{p}, \mathbf{y}, T)$ 
10:     $aux \leftarrow e^{(l^{(t+1)} - l^{(t)})} q(\mathbf{L}_{(t-1,:)}) / q(\mathbf{p})$ 
11:     $l^{(t)} \leftarrow l^{(t+1)}$ 
12:    if  $\min\{aux, 1\} < 1$  then
13:       $\mathbf{L}_{(t,:)} \leftarrow \mathbf{L}_{(t-1,:)}$ 
14:    else
15:       $\mathbf{L}_{(t,:)} \leftarrow \mathbf{p}$ 
16:    end if
17:  end for
18:  return  $\mathbf{L}$ 
19: end function

```

each parameter α_j in \mathbf{p} , an independent log-normal distribution was used such that $q(\mathbf{p}^{new} | \mathbf{p}^{old}) = \prod_{j=0}^3 q(\mathbf{p}_j^{new} | \mathbf{p}_j^{old})$, with $q(\mathbf{p}_j^{new} | \mathbf{p}_j^{old}) = \log\mathcal{N}(\ln(\mathbf{p}_j^{old}), \sigma_j^2)$, where the standard deviations σ_j , $j = 0, \dots, 3$ were establish as 10 times the average of the prior distribution. Proposed parameter samples are accepted with probability

$$p_r = \min \left\{ 1, \frac{\mathcal{P}(\mathbf{p}^{new} | \mu_0, \dots, \mu_3) q(\mathbf{p}^{old} | \mathbf{p}^{new})}{\mathcal{P}(\mathbf{p}^{old} | \mu_0, \dots, \mu_3) q(\mathbf{p}^{new} | \mathbf{p}^{old})} \right\}. \quad (12)$$

From the resulting Markov chain, we extracted the parameter configuration which maximized the posterior density.

6. SIMULATIONS AND RESULTS

Simulations were conducted to show the performance of the boolean coded aperture designs to recover the phase from diffracted pattern measurements. The value of the transmittance t_r and the number of required projections L were varied $0.1 \leq t_r \leq 0.9$ ($0.1 \leq t_r \leq 0.5$ in case of Hadamard and blue noise patterns) and $2 \leq L \leq 15$ with a step size 0.1 and 1 respectively, in order to determine their optimal value. The optimal transmittance is the minimum value of t_r when the quality of reconstruction does not increase with the number of projections. On the other hand, the required number of projections is the minimum value of L when the quality of reconstruction does not increase.

To simulate the acquisition process, a set of synthetic images in phase was built as follow. Let $\mathbf{A} = (a_{kj}) \in \mathbb{R}^{n \times n}$ and $\mathbf{B} = (b_{kj}) \in \mathbb{R}^{n \times n}$ be images. Based on the polar form of a complex number, then an image $\mathbf{V} = (v_{kj}) \in \mathbb{C}^{n \times n}$ is given by $v_{kj} = a_{kj}e^{-i\pi b_{kj}}$ where a_{kj} and b_{kj} are the magnitude and the phase of the complex number v_{kj} respectively. Thus, the images \mathbf{A} and \mathbf{B} are the magnitude and the phase of image \mathbf{V} respectively.

The optimal truncation parameters were found with Algorithm 2, which results in $\alpha_0 = 0.045$, $\alpha_1 = 5$, $\alpha_2 = 6$ and $\alpha_3 = 3$. Moreover, there were a significant reduction of the variances of the prior distributions, that is, 35%, 25%, 28% and 40% for the truncation parameters α_j , $j = 0, \dots, 3$ respectively.

All experiments were carried out on Matlab 2015a on an Intel Core i7-4790 3.6 GHz x 8 with 32 GB RAM memory. The presented results are the average of 100 realizations for each case. Finally, the performance of the boolean coded apertures was measured with the Peak-Signal-to-Noise-Ratio (PSNR) metric.

6.1. Optimal design parameters for boolean coded apertures

Figure 2 shows the obtained results for transmittance and number of required projections using different boolean coded apertures in recovering the phase. According to the obtained performance, the minimum number of t_r such that the quality of reconstruction does not increase with the number of projections is 0.5, *i.e.* the optimal transmittance value for boolean coded apertures in recovering the phase is 50%. Notice that the minimum number of projections (MP), when the quality of reconstruction does not increase, depends on the coded aperture design. Using Hadamard coded apertures the MP is $L = 7$ and in the case of random designs MP is $L = 8$, $L = 6$ and $L = 4$ using DFT and blue noise patterns, respectively.

6.2. Reconstructions

Figure 3 shows the reconstructed images in recovering the phase using the different types of boolean coded apertures and the STWF reconstruction algorithm. This experiment used the optimal transmittance *i.e.* $t_r = 0.5$ and the number of

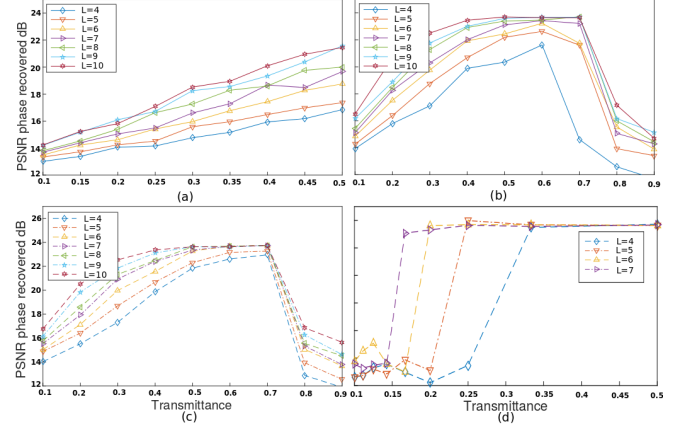


Fig. 2: Analysis of transmittance and number of required projections. (a) Hadamard structures, (b) random coded apertures, (c) DFT coded apertures and (d) blue noise patterns.

required projections $L = 5$. Notice that the highest performance in recovering the phase is obtained with the blue noise patterns. These results show that the blue noise patterns require less number of projections than the other designs. Then, we conclude that the spatial distribution is an important design parameter in boolean coded apertures.

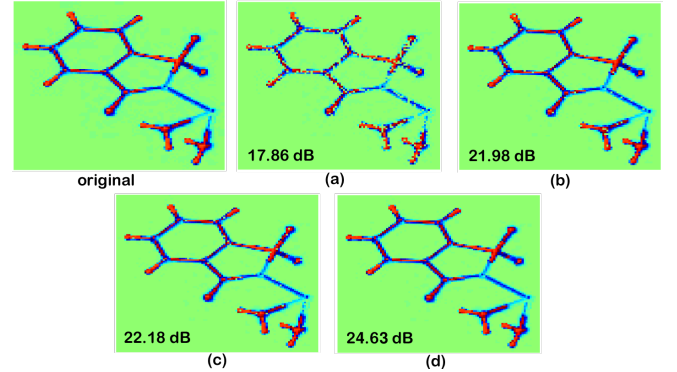


Fig. 3: Phase reconstructions using (a) Hadamard coded apertures, (b) random coded apertures, (c) coded apertures with DFT and (d) coded apertures with blue noise pattern.

7. CONCLUSIONS

The STWF algorithm for recovering the phase from intensity of diffracted and patterned X-rays measurement using boolean coded apertures was presented. The effect of different types of boolean coded apertures has been studied. Simulations indicate that optimal transmittance for the boolean coded apertures is 50%. Moreover, the quality of the reconstructions using boolean coded apertures attained up to 24.63dB of PSNR. The blue noise patterns provide better reconstruction quality than other presented boolean designs. Ultimately, choosing the correct truncation parameters of the STWF algorithm and changing the initialization strategy allowed to solve the phase retrieval problem using boolean coded apertures.

8. REFERENCES

- [1] M. Smyth and J. Martin, "x ray crystallography," *Journal of Clinical Pathology*, vol. 53, no. 1, pp. 8, 2000.
- [2] J. Drenth, *Principles of protein X-ray crystallography*, Springer Science & Business Media, 2007.
- [3] R. Cernik, W. Clegg, R. Catlow, G. Bushnell, J. Flaherty, N. Greaves, I. Burrows, D. Taylor, S. Teat, and M. Hamichi, "A new high-flux chemical and materials crystallography station at the srs daresbury. 1. design, construction and test results. corrigendum," *Journal of Synchrotron Radiation*, vol. 7, no. 1, pp. 40–40, 2000.
- [4] E. Candes, X. Li, and M. Soltanolkotabi, "Phase retrieval from coded diffraction patterns," *Applied and Computational Harmonic Analysis*, vol. 39, no. 2, pp. 277–299, 2015.
- [5] E. Candes, X. Li, and M. Soltanolkotabi, "Phase retrieval via wirtinger flow: Theory and algorithms," *IEEE Transactions on Information Theory*, vol. 61, no. 4, pp. 1985–2007, 2015.
- [6] Y. Chen and E. Candes, "Solving random quadratic systems of equations is nearly as easy as solving linear systems," in *Advances in Neural Information Processing Systems*, 2015, pp. 739–747.
- [7] E. Candes, Y. Eldar, T. Strohmer, and V. Voroninski, "Phase retrieval via matrix completion," *SIAM review*, vol. 57, no. 2, pp. 225–251, 2015.
- [8] S. Pinilla and H. Arguello, "Phase recovery from diffraction patterns using boolean coded apertures and the truncated wirtinger flow algorithm," in *Imaging and Applied Optics 2016*. 2016, p. JT3A.28, Optical Society of America.
- [9] K. MacCabe, A. Holmgren, M. Tornai, and D. Brady, "Snapshot 2d tomography via coded aperture x-ray scatter imaging," *Applied optics*, vol. 52, no. 19, pp. 4582–4589, 2013.
- [10] J. Greenberg, K. Krishnamurthy, M. Lakshmanan, K. MacCabe, S. Wolter, A. Kapadia, and D. Brady, "Coding and sampling for compressive x-ray diffraction tomography," in *SPIE Optical Engineering+ Applications*. International Society for Optics and Photonics, 2013, pp. 885813–885813.
- [11] A. Cuadros, C. Peitsch, H. Arguello, and G. Arce, "Coded aperture optimization for compressive x-ray tomosynthesis," *Opt. Express*, vol. 23, no. 25, pp. 32788–32802, Dec 2015.
- [12] B. Rodriguez, G. Arce, and D. Lau, "Blue-noise multi-tone dithering," *IEEE Transactions on Image Processing*, vol. 17, no. 8, pp. 1368–1382, 2008.